J Biomol NMR (2014) 60:37–44
DOI 10.1007/s10858-014-9848-9

ARTICLE

Comparison of the sensitivities of WaterLOGSY and saturation transfer difference NMR experiments

Aleksandar Antanasijevic · Benjamin Ramirez · Michael Caffrey

Received: 28 April 2014 / Accepted: 8 July 2014 / Published online: 12 July 2014

Abstract The WaterLOGSY (WL) and saturation transfer difference (STD) NMR experiments have proven to be extremely useful techniques to characterize interactions between small molecules and large biomolecules. In this work we compare the relative sensitivities of WL and STD NMR using 3 experimental systems: ketoprofen (KET)–bovine serum albumin (BSA), *tert*-butyl hydroquinone (TBHQ)–hemagglutinin (HA), and chloramphenicol (CAM)–ribosome (70S). In all cases we find that WL is more sensitive than STD for a given experimental time with the ratios ranging from 3.2 for KET–BSA to 16 for TBHQ–HA and CAM–70S. We attribute the increased sensitivity of WL to be due to simultaneous saturation of multiple sources of cross correlation, including direct NOEs of ^{1}H of water and exchangeable groups and indirect NOEs of ^{1}H–C groups. We suggest that the outstanding sensitivity of WL make it ideally suited for drug screening efforts targeting very large biomolecules at relatively low concentrations.

Keywords BSA · Hemagglutinin · Ribosome · STD · WaterLOGSY

Introduction

NMR has proven to be a powerful technique to characterize interactions between small molecules and large biomolecules (Carlomagno 2005; Williamson 2009; Harner et al. 2013). The biomolecules understudy may consist of proteins, DNA, RNA, and carbohydrates. The small molecules, termed ligands hereafter, may consist of natural ligands (e.g. substrates, products, receptors, inhibitors or activators), where NMR studies give insights into function, or drug-like molecules, in which NMR studies enable discovery and optimization of potency. NMR characterizations may occur via target-based (i.e. biomolecule) or ligand-based techniques. Target-based techniques employ chemical shift perturbations of the biomolecule and in some cases intermolecular NOEs between the ligand and target. Such experiments present the potential to not only identify binding (and affinity) but also the interaction site and, in favorable cases, the structure of the ligand–biomolecule complex (Shuker et al. 1996). However, target-based techniques require relatively large amounts of highly purified biomolecule (i.e. mg quantities), as well as labeling with stable isotopes (typically ^{13}C and/or ^{15}N), and are limited to relatively small molecular weight biomolecules (e.g. <50 kDa). On the other hand, ligand based techniques take advantage of relatively fast exchange between the bound and free ligand, which is often the case in biological systems (i.e. $k_{off} > 100\ s^{-1}$ or $K_d > 0.1\ \mu M$, Williamson 2009). In the case of fast exchange and excess ligand, ligand-based techniques exhibit higher sensitivity due to narrower line-widths and multiple binding events, as well as lower spectral ambiguities (i.e. fewer signals). Moreover, ligand-based techniques present the potential to utilize smaller quantities, as well as unpurified samples, of targeted biomolecules, and labeling with stable isotopes is unnecessary. However, ligand based techniques require additional experiments to identify the binding site (e.g. competition assays with ligands of known binding sites, mutagenesis of the target biomolecule, or high resolution X-ray structures).

A. Antanasijevic · B. Ramirez · M. Caffrey (✉)
Department of Biochemistry and Molecular Genetics, University of Illinois at Chicago, 900 S Ashland Ave, Chicago, IL 60607, USA
e-mail: caffrey@uic.edu

WaterLOGSY (WL) and saturation transfer difference (STD) are two popular ligand-based NMR experiments used to characterize interactions of small molecules with biomolecules (Dalvit et al. 2001; Mayer and Meyer 2001). Both WL and STD are based on intermolecular NOEs to the transiently bound ligand ^{1}H. In the case of WL, ^{1}H of bulk water is excited and magnetization is transferred from transiently bound water ^{1}H to bound ligand ^{1}H (Dalvit et al. 2000, 2001). Note that magnetization transfer to the bound ligand ^{1}H may also occur via indirect spin diffusion through exchangeable and nonexchangeable ^{1}H of the biomolecule and that exchangeable ^{1}H of ligands cannot be used as probes in WL (Dalvit et al. 2000, 2001). In the case of STD, a selected ^{1}H spectral region of the biomolecule is saturated in the "on" resonance experiment (e.g. the methyl ^{1}H that resonate near 0 ppm), additional biomolecule ^{1}H are saturated via efficient spin diffusion that occurs in large biomolecules, and an intermolecular NOE occurs from biomolecule ^{1}H that are proximal to the binding site (<6 Å) to the small molecule ^{1}H (Mayer and Meyer 2001). A second experiment is performed in which a region far from the biomolecule spectral range is saturated, the "off" resonance experiment, and the difference spectrum of the "on" and "off" experiments reveals the magnetization transfer from the biomolecule to individual ligand ^{1}H. In what follows, we have compared the relative sensitivities of the WL and STD experiments for three ligand–biomolecule systems: ketoprofen (KET)–bovine serum albumin (BSA), *tert*-butylhydroquinone (TBHQ)–hemagglutinin (HA), and chloramphenicol (CAM)–ribosome (70S), with the goal of determining the optimal NMR-experiments for the characterization of ligand–biomolecule interactions in relatively large molecular weight systems.

Materials and methods

BSA, CAM, KET, and TBHQ were obtained from Sigma. H3 HA Brisbane (full-length) was obtained from BEI Resources. Ribosome 70S was prepared as previously described (Belova et al. 2001). All NMR experiments were performed on Bruker 800 and 900 MHz Avance spectrometers, the latter equipped with a cryogenic triple resonance probe. The experimental conditions for the KET–BSA experiments were ±10 μM BSA, 300 μM KET, 20 mM PBS/pH 7.4, 150 mM NaCl and 10 % ^2H_2O at 25 °C. The experimental conditions for the TBHQ–HA experiments were ±0.5 μM HA, 300 μM TBHQ, 20 mM PBS/pH 7.4, 150 mM NaCl and 10 % ^2H_2O at 25 °C. The experimental conditions for the CAM–70S experiments were ±0.5 μM 70S, 300 μM CAM, 25 mM d-Tris–HCl/pH 7.4, 150 mM KCl, 5 mM $MgCl_2$, 2 mM BME and 10 % ^2H_2O at 25 °C. The 20-fold higher concentration of BSA with respect to HA and 70S was chosen to give similar S/N in the WL and STD experiments. WL experiments were performed as previously described (Dalvit et al. 2001; Ramirez et al. 2014). Water was inverted using a 10 ms iBurp2 pulse followed by a 1 or 2 s mixing time and a relaxation delay of 2.5 s. The total number of scans was set to 3,072 and the total acquisition time was ~6 h. STD experiments were performed as described previously (Mayer and Meyer 2001; McCullough et al. 2012). Here, unless otherwise noted the protein ^{1}H were saturated with a train of 50 ms Gaussian-shaped pulses at a field strength of 100 Hz for 1 or 2 s with "on" resonance saturation at −0.5 ppm and "off" resonance saturation at 40 or 50 ppm and a relaxation delay of 2.5 s. The total number of scans was set to 6,144 and the total acquisition time was ~12 h. For the STD experiments a second control experiment was performed in the absence of biomolecule to ensure that ligand resonances were not being excited. In the case of the WL experiment, the signal intensities were determined after subtracting the control experiment (with ligand alone). For the protein saturation experiments, WL was performed as the difference between spectra acquired with water ^{1}H inversion (i.e. −z axis) and that acquired in which water ^{1}H remained in the +z axis. The STD protein saturation experiments were performed as described above. For the protein saturation experiments, the experimental conditions were 40 μM BSA in 20 mM PBS/pH 7.4, 150 mM NaCl and 10 % ^2H_2O or 100 % ^2H_2O at 25 °C. Spectra were processed by NMRPipe using a 5 Hz line broadening function and subsequently analyzed by NMRDraw (Delaglio et al. 1995). In all cases, noise levels for the final spectra were estimated by NMRDraw and errors were calculated as previously described (McCullough et al. 2012).

Results and discussion

To compare the sensitivities it is important to present the details for the WL and STD NMR experiments. For these experiments we chose standard pulse sequences depicted in Fig. 1a (Dalvit et al. 2001; Mayer and Meyer 2001), which we have found to be relatively easy to implement and robust for studies designed to discover drug-like ligands, characterize their interaction, and guide chemical improvement (Celigoy et al. 2011; McCullough et al. 2012; Antanasijevic et al. 2013; Basu et al. 2013; Ramirez et al. 2014). It is also important to determine the experimental protocol to be used to fairly compare the two experiments. In this case we chose to make the total experimental time periods of the WL and STD experiments to be the same (i.e. each experiment was set up to take a total time of

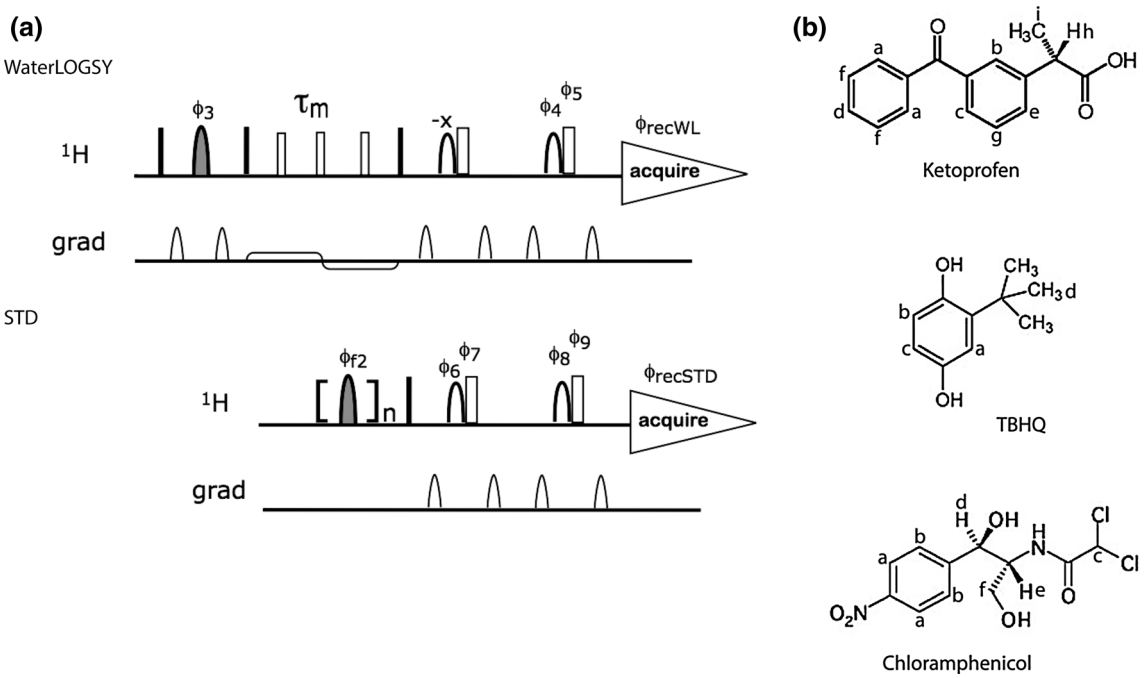

Fig. 1 **a** Pulse sequence diagrams for the STD and WaterLOGSY experiments with water suppression by the double-pulsed field gradient spin echo method. The *solid bars* and *boxes* represent hard 90° and 180° rf pulses, respectively. For STD after the initial d1 relaxation delay, proton magnetization is saturated either on or off resonance by a train of 50 ms Gauss pulses, indicated by the *shaded shaped pulse* in *brackets*. Typical saturation times are 1–2 s. In the final two echo periods, the shaped 180° pulse has a sinc shape with a duration of 2.2 ms; gradient strengths are 12 and 15 G/cm, respectively. For WaterLOGSY, these same parameters are used. The *shaded shaped pulse* is a 10 ms iBurp2 pulse that selectively inverts water magnetization; the gradients surrounding this pulse has a strength of ~20 G/cm. The mixing period (τ_m) is usually 1 or 2 s in duration; during this period a weak bipolar gradient is applied to suppress radiation damping. Also, hard 180° pulses are applied in the mixing period to remove artifacts. For both experiments, d1, the relaxation delay, is 2.5 s, and the total acquisition time is ~4 s. Phase cycling: ϕ_3 = x, −y, −x, y; ϕ_4 = −x, −x, −x, −x, y, y, y, y, x, x, x, x, −y, −y, −y, −y; ϕ_5 = x, x, x, x, −y, −y, −y, −y, −x, −x, −x, −x, y, y, y, y; ϕ_{recWL} = x, −x, x, −x, −x, x, x, −x; ϕ_{f2} = x; ϕ_6 = x, x, y, y; ϕ_7 = −x, −x, −y, −y; ϕ_8 = x, x, x, x, y, y, y, y; ϕ_9 = −x, −x, −x, −x, −y, −y, −y, −y; ϕ_{recSTD} = x, −x, −x, x, −x, x, x, −x. All other rf pulses are applied with phase along the x-axis. The pulse sequence program for the WaterLOGSY experiment is available from the authors by request. **b** Ligands used in this study with the ^{1}H nomenclature shown

12 h) with identical relaxation times, saturation times, and receiver gain values. As noted in the introduction, STD is a difference experiment that requires acquisition of one scan "on" resonance (i.e. selective excitation of the biomolecule ^{1}H) and a second scan "off" resonance (i.e. excitation in a region far from any biomolecule ^{1}H). Accordingly, we chose to run the WL experiments in a difference mode in which 50 % of the experimental time used a sample containing the ligand and biomolecule (6 h total) and 50 % of the experimental time used a second sample containing only the ligand (6 h total). We note that this approach is generally useful in the WL experiment because the ligand resonances, in the absence of biomolecule, are often of the opposite sign of those in the presence of the biomolecule and thus this control experiment is useful to avoid confusion between ligands that bind and those that do not bind (c.f. Ramirez et al. 2014). Moreover, in WL the exchangeable ^{1}H of the ligand are often the opposite sign of the nonexchangeable ^{1}H in the absence of biomolecule and thus the difference spectra removes them from consideration.

For these studies we have chosen three ligand–biomolecule systems, in which the molecular weights of the biomolecules are >50 kDa, a realm where ligand-based methods present distinct advantages to target-based methods (Carlomagno 2005). Moreover, both the WL and STD experiments are based on an intermolecular NOE and the maximum NOE is expected to occur at $\tau_c > 10$ ns (Williamson 2009) and thus all three systems are expected to exhibit optimal NOE efficiency. The first system under study is that of the KET–BSA interaction. This interaction is of physiological significance because KET is a widely prescribed NSAID, which is transported in plasma via its interaction with HSA, the human analog of BSA (Bi et al. 2010). BSA is a 67 kDa monomer with an estimated $\tau_c \sim 40$ ns and the K_d of its interaction with KET is ~0.3 μM (Sowell et al. 2001). The second system under study is that of the TBHQ–HA interaction. TBHQ is a

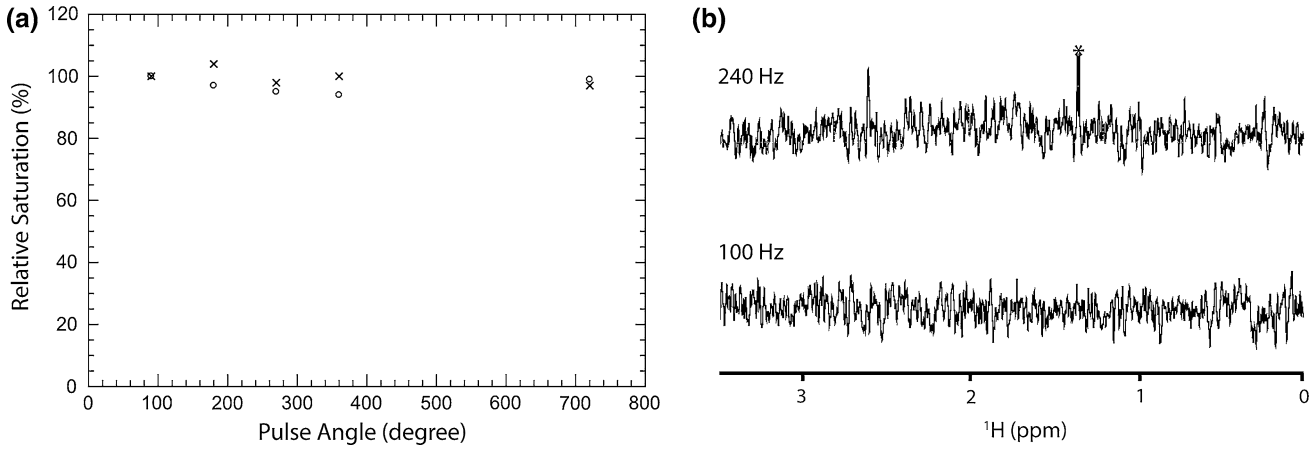

Fig. 2 **a** Protein saturation using Gaussian selective pulses of various angles at field strength of 100 Hz and 2 s of total saturation time. The saturation pulses correspond to 6.25, 12.5, 18.75, 25, and 50 ms, which correspond to pulse angles of 90°, 180°, 270°, 360° and 720°, respectively. Relative saturation for the downfield (>4.7 ppm, *times symbol*) and upfield (<4.7 ppm, *open circle*) spectral regions were estimated using the TopSpin 3.2. The experimental conditions were 40 μM BSA in 20 mM PBS/pH 7.4, 150 mM NaCl and 10 % ^2H_2O at 25 °C. **b** STD saturation of ligand in the absence of biomolecule at field strengths of 100 and 240 Hz with the KET resonance denoted by an asterisk. Experimental conditions were 300 μM KET in 20 mM PBS/pH 7.4, 150 mM NaCl and 10 % ^2H_2O at 25 °C

promising small molecule inhibitor of influenza entry that binds to the stem loop region of HA (Antanasijevic et al. 2013). HA is a 210 kDa trimer with an estimated $\tau_c \sim 120$ ns and the K_d of its interaction with TBHQ is ~6 μM (Antanasijevic et al. 2013). The final system under study is that of the CAM–70S interaction. This interaction is of physiological significance in that CAM is considered as the prototypical broad-spectrum antibiotic that targets the peptidyl transferase site of the ribosome (Schlünzen et al. 2001). In contrast to the other systems under study, 70S is a complex of RNA and protein subunits with a molecular weight of 2,500 kDa, an estimated $\tau_c \sim 1{,}500$ ns, and the K_d of its interaction with CAM is ~2 μM (Mamos et al. 2013). For reference, the structures of the ligands and ^{1}H nomenclature used herein are shown in Fig. 1b.

Finally, it is of interest to consider the protein saturation to be achieved in the STD experiment, which will be a function of frequency and field strength of the selective saturation pulses (Mayer and Meyer 2001; Cutting et al. 2007; Ley et al. 2014). With respect to the frequency we have chosen a standard value of −0.5 ppm for the "on" frequency, which is a balance between achieving selective saturation of protein ^{1}H and not ligand ^{1}H at a particular saturation field strength. With respect to the field strength of the selective saturation pulses, it has recently been shown that the resulting STD signal is insensitive to the pulse angle at a given field strength (Cutting et al. 2007). To test this observation, we compared the relative signal intensities of the downfield and upfield spectral regions of BSA using different Gaussian pulse angles at a field strength of 100 Hz in the STD experiment without ligand. As shown in Fig. 2a, no significant differences in protein saturation are observed for pulse angles ranging from 90° to 720°. We next tested the use of higher power selective pulses, which have recently been shown to increase S/N of the STD experiment in select cases (Cutting et al. 2007; Ley et al. 2014). Consequently, we compared the saturation of BSA in the STD experiment using selective Gaussian pulses with a field strength of 240 versus the 100 Hz power used in the above experiment. We found that increasing the power to 240 Hz did indeed increase the protein saturation by a factor of ~3.5 (data not shown); however, as shown in Fig. 2b the increased power resulted in an unacceptable amount of ligand excitation, which would require an additional STD control experiment on ligand alone, thereby increasing experimental times by a factor of 2. Thus, we feel that selective pulses with field strengths of 100 Hz offer the optimal combination of saturation efficiency and selectivity in the STD experiment.

In the next step, we carefully compared the STD and WL signals for biomolecule–ligand interactions for our 3 systems. In Fig. 3, we give examples of the STD and WL spectra with 1 and 2 s saturation or mixing times, respectively. First note that increasing the saturation or mixing time from 1 to 2 s does not appear to significantly change the signal intensities observed in both the STD and WL experiments, suggesting that by 1 s we are observing maximal signals. Importantly, it is obvious that for a given amount of experimental time that the WL experiment is significantly more sensitive than the STD experiment for all 3 systems, which range from 67 to 2,500 kDa.

We next quantified the differences in the S/N of the STD and WL spectra for different ligand resonances in Fig. 4 and Table 1. Note that we assume that we are monitoring

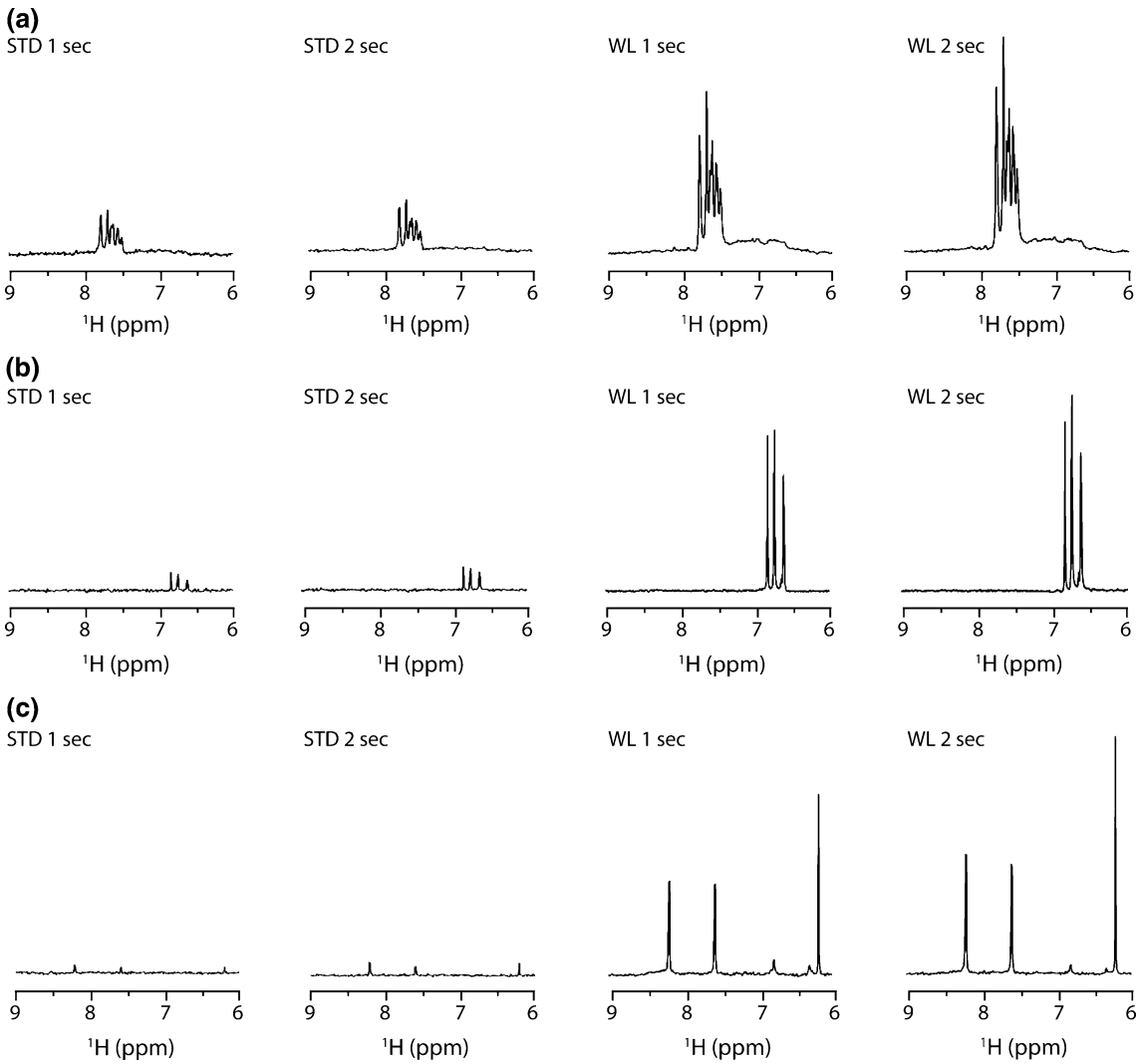

Fig. 3 Examples of WaterLOGSY and STD spectra used to compare sensitivities for **a** KET–BSA, **b** TBHQ–HA and **c** CAM–ribosome 70S. In all cases the relaxation delays, saturation/mixing times, receiver gain and total experimental times were identical

the same binding event in both experiments (i.e. the same site with the same ligand residence time). Consequently, individual differences in T1, T2 and intramolecular spin diffusion for ^{1}H within a particular ligand are expected to not be relevant when comparing the ratio of the 2 experiments at the same saturation or mixing times. In the case of KET–BSA, the ratio of WL–STD sensitivity ranges from 3.3 to 3.7 with averages of 3.2 ± 0.1 and 3.5 ± 0.2 for the 1 and 2 s experiments, respectively. In the case of TBHQ–HA, the ratio of WL–STD sensitivity ranges from 11 to 19 with averages of 16 ± 4 and 12 ± 5 for the 1 and 2 s experiments, respectively. In the case of CAM–70S, the ratio of WL to STD sensitivity ranges from 8.9 to 23 with averages of 16 ± 9 and 14 ± 6 for the 1 and 2 s experiments, respectively. Recently, it has been shown that "off" saturation at 50 ppm is not appropriate for very large biomolecules (e.g. viruses) due to large ^{1}H linewidths (Rademacher et al. 2008). Accordingly, we performed an additional STD experiment on the CAM–70S system using "off" saturation at 300 ppm. In this case, there were no significant differences in the intensities of the ligand resonances, suggesting that the STD experiment was not attenuated by the use of an inappropriate "off" frequency (data not shown).

Interestingly, the sensitivities of the KET–BSA signals are relatively uniform in contrast to the TBHQ–HA and CAM–70S sensitivities. As noted in the introduction, the STD signal comes from magnetization transfer from biomolecule ^{1}H and the WL signal comes from magnetization transfer from transiently bound water ^{1}H or indirectly via nonexchangeable and exchangeable ^{1}H of biomolecules. Consequently, relatively lower WL to STD sensitivity would be expected for ligand ^{1}H in close proximity to hydrophobic regions of the biomolecule (e.g. with methyl

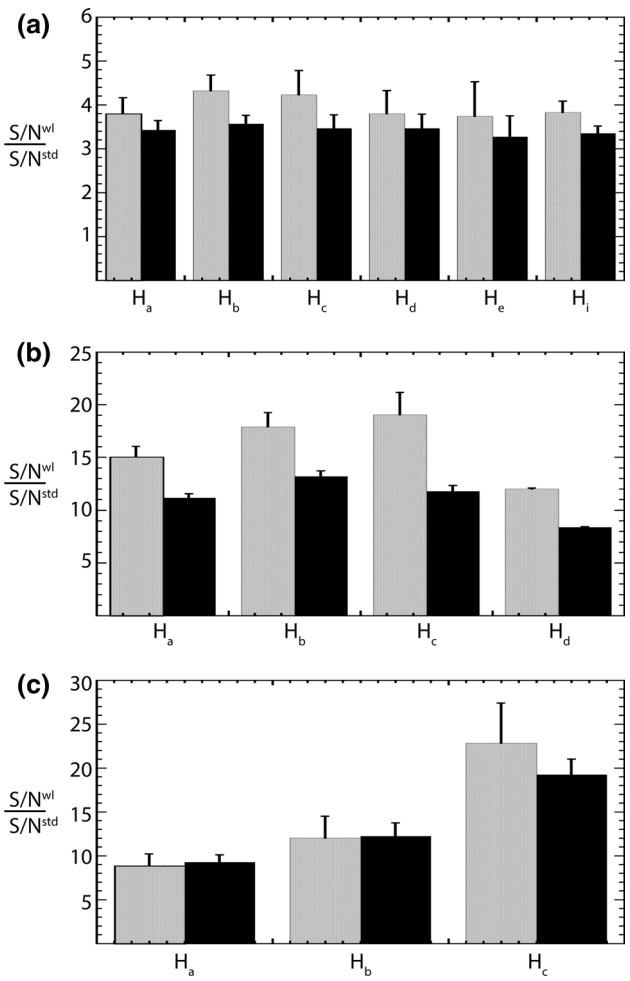

Fig. 4 Quantified differences in sensitivities of individual resonances in the WaterLOGSY and STD NMR experiments. Resonances follow the nomenclature presented in Fig. 1b. *Light bars* represent 1 s saturation/mixing times and *dark bars* represent 2 s saturation/mixing times. *Error bars* have been estimated from the noise of the final spectra as in McCullough et al. (2012)

Table 1 Average $S/N^{wl}/S/N^{std}$

System	$S/N^{wl}/S/N^{std}$ (1 s)	$S/N^{wl}/S/N^{std}$ (2 s)	n
KET–BSA	3.22 ± 0.12	3.45 ± 0.17	6
TBHQ–HA	15.6 ± 4.1	11.8 ± 5.4	4
CAM–ribosome 70S	16.2 ± 8.6	14.2 ± 5.9	3

or aromatic groups) and relatively higher WL–STD sensitivity would be expected for ligand ^{1}H in close proximity to transiently bound water or exchangeable groups of the biomolecule (i.e. hydrophilic regions). Thus, it is not surprising that the ratio of sensitivities varies for the ^{1}H of a particular ligand. Nonetheless, we find that WL is more sensitive than STD for all ligand ^{1}H in all of the model systems studied. We note, however, that the STD signal has been reported to be increased on the order of $\sim 2\times$ by running the experiments in 100 % ^2H_2O, due to reduced spin diffusion between the biomolecule ^{1}H and bulk water ^{1}H (Mayer and James 2002; Cutting et al. 2007). Accordingly, we performed the STD experiments in 100 % ^2H_2O for our larger 2 systems (TBHQ–HA and CAM–70S). We found that the STD signals increased by a factor of ~ 6–$7\times$ (data not shown); however, the WL experiments remain significantly more sensitive, suggesting that only part of the sensitivity difference can be achieved in 100 % ^2H_2O. Moreover, a number of recent improvements to the WL experiment have been reported to achieve S/N gains of $\sim 2\times$ (Gossert et al. 2009). Finally, we note that buffer substitution will not always be feasible for labile or ex vivo systems (e.g. viruses or cells).

The differences in relative sensitivity between WL and STD could be due to a number of factors including the efficiency of protein saturation or partial excitation of biomolecule ^{1}H that resonate near ^1H_2O (e.g. $^1H_\alpha$). To test the relative efficiency of protein saturation we compared the STD signal of BSA in the absence of ligand to the difference spectra between a WL experiment in which water ^{1}H were inverted to the $-$z axis and a second WL experiment in which water ^{1}H remained along the $+$z axis. As shown in Fig. 5a, the upfield spectral region of BSA exhibits significantly more saturation in the WL experiment than the STD experiment for identical experimental conditions. Moreover, the WL experiment appears to achieve more uniform saturation within the biomolecule. Taken together, this observation suggests that the higher S/N of the WL is at least partially due to indirect magnetization transfer via biomolecule ^{1}H to ligand ^{1}H. Next, we performed assessed the effect of partial saturation of $^1H_\alpha$ in the WL sequence by performing the experiment in 100 % ^2H_2O. As shown by Fig. 5b, no detectable saturation of BSA is achieved in the absence of ^1H_2O and thus the protein saturation of the WL experiment is clearly mediated by ^1H_2O (and possibly exchangeable ^{1}H), as previously noted by Dalvit et al. (2001).

In conclusion, we reiterate that sensitivity in the NMR characterizations of biomolecule interactions with ligands is extremely important. For example, higher sensitivity reduces experimental times, which enables study of unstable systems, increases throughput and spectrometer efficiency, decreases the need for ultrahigh field spectrometer time, and enables kinetic studies. Moreover, the WL and STD experiments are optimal for excess ligands in relatively fast exchange and thus the sensitivity of the experiment is proportional to the biomolecule concentration. This becomes limiting when there are small amounts of biomolecule available due to difficulties in obtaining mg quantities, low natural concentrations, and/or complex systems that are difficult to isolate (e.g. membrane proteins

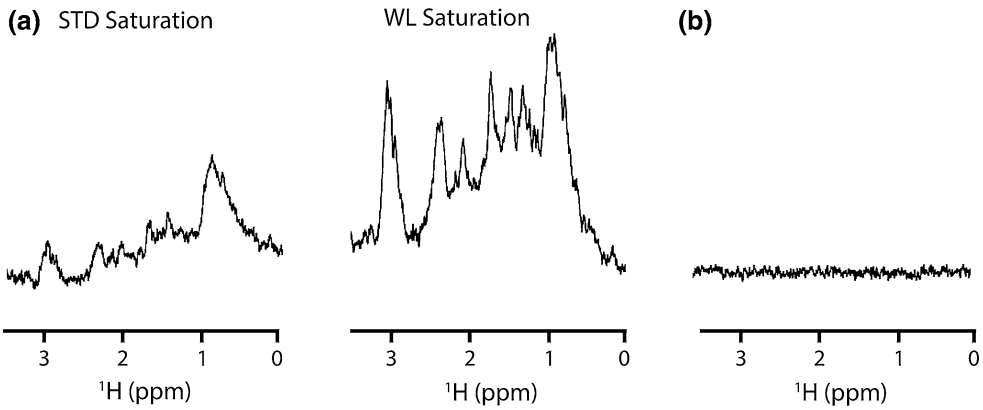

Fig. 5 Comparison of BSA saturation efficiencies. **a** Relative protein saturation using STD saturation at 100 Hz power and WaterLOGSY saturation. **b** Relative protein saturation using WaterLOGSY saturation in the absence of water ^{1}H. The experimental conditions were 40 μM BSA in 20 mM PBS/pH 7.4, 150 mM NaCl and 10 % ^2H_2O in **a** and 100 % ^2H_2O in **b** at 25 °C

present in a viral or cellular membrane). In addition, increased sensitivity allows characterizations of ligands at lower concentrations nearer the K_d, which is important when there is the potential for additional lower affinity binding sites. We find that WL is generally more sensitive and importantly requires less attention to saturation power and the determination of the optimal "on" resonance saturation frequency, which is particularly important for NMR-based drug screens. Nonetheless, the STD experiment gives unique insight into the proximity of ligand ^{1}H to the biomolecule surface and thus STD will continue to be an important component of the spectroscopist's toolkit. Finally, we note that STD has been applied to membrane-bound systems at relatively low concentrations (Assadi-Porter et al. 2010) and thus WL experiments on such systems are expected to be >10× more sensitive, thereby allowing increased numbers of membrane systems to be characterized by NMR.

Acknowledgments The authors would like to gratefully thank Alexander Mankin for the kind gift of purified ribosome-70S. This work was supported by NIH Grant R21AI101676 and the UIC Research Resources Center and the Center for Structural Biology.

References

Antanasijevic A, Cheng H, Wardrop D, Rong L, Caffrey M (2013) Inhibition of influenza H7 hemagglutinin-mediated entry. PLoS One 8:e76363

Assadi-Porter FM, Tonelli M, Maillet EL, Markley JL, Max M (2010) Interactions between the human sweet-sensing T1R2–T1R3 receptor and sweeteners detected by saturation transfer difference NMR spectroscopy. Biochim Biophys Acta 1798:82–86

Basu A, Antanasijevic A, Wang M, Li B, Mills D, Ames J, Moir DT, Prichard M, Barnard DL, Caffrey M, Rong L, Bowlin TL (2013) Novel inhibitors of influenza A virus fusion: interaction with the viral hemagglutinin. J Virol 88:1447–1460

Belova L, Tenson T, Xiong L, McNicholas PM, Mankin AS (2001) A novel site of antibiotic action in the ribosome: interaction of evernimicin with the large ribosomal subunit. Proc Natl Acad Sci USA 98:3726–3731

Bi S, Yan L, Sun Y, Zhang H (2010) Investigation of ketoprofen binding to human serum albumin by spectral methods. Spectrochim Acta A Mol Biomol Spectrosc 78:410–414

Carlomagno T (2005) Ligand–target interactions: what can we learn from NMR? Annu Rev Biophys Biomol Struct 34:245–266

Celigoy J, Ramirez B, Tao L, Rong L, Yan L, Feng YR, Quinnan GV, Broder CC, Caffrey M (2011) Probing the HIV gp120 envelope glycoprotein conformation by NMR. J Biol Chem 286:23975–23981

Cutting B, Shelke SV, Dragic Z, Wagner B, Gathje H, Kelm S, Ernst B (2007) Sensitivity enhancement in saturation transfer difference (STD) experiments through optimized excitation schemes. Magn Reson Chem 45:720–724

Dalvit C, Pevarello P, Tatò M, Veronesi M, Vulpetti A, Sundström M (2000) Time efficient detection of protein-ligand interactions with the polarization optimized PO-WaterLOGSY NMR experiment. J Biomol NMR 18:65–68

Dalvit C, Fogliatto G, Stewart A, Veronesi M, Stockman B (2001) WaterLOGSY as a method for primary NMR screening: practical aspects and range of applicability. J Biomol NMR 21:349–359

Delaglio F, Grzesiek S, Vuister GW, Zhu G, Pfeifer J, Bax A (1995) NMRPipe: a multidimensional spectral processing system based on UNIX pipes. J Biomol NMR 6:277–293

Gossert AD, Henry C, Blommers MJ, Jahnke W, Fernández C (2009) Time efficient detection of protein–ligand interactions with the polarization optimized PO-WaterLOGSY NMR experiment. J Biomol NMR 43:211–217

Harner MJ, Frank AO, Fesik SW (2013) Fragment-based drug discovery using NMR spectroscopy. J Biomol NMR 56:65–75

Ley NB, Rowe ML, Williamson RA, Howard MJ (2014) Optimising selective excitation pulses to maximize saturation transfer difference NMR spectroscopy. RSC Adv 4:7347–7351

Mamos P, Krokidis MG, Papadas A, Karahalios P, Starosta AL, Wilson DN, Kalpaxis DL, Dinos GP (2013) On the use of the antibiotic chloramphenicol to target polypeptide chain mimics to the ribosomal exit tunnel. Biochimie 95:1765–1772

Mayer M, James TL (2002) Detecting ligand binding to a small RNA target via saturation transfer difference NMR experiments in D_2O and H_2O. J Am Chem Soc 24:13376–13377

Mayer M, Meyer B (2001) Group epitope mapping by saturation transfer difference NMR to identify segments of a ligand in direct contact with a protein receptor. J Am Chem Soc 123:6108–6117

McCullough C, Wang M, Rong L, Caffrey M (2012) NMR characterization of influenza hemagglutinin receptor interactions. PLoS One 7:e33958

Rademacher C, Krishna NR, Palcic M, Parra F, Peters T (2008) NMR experiments reveal the molecular basis of receptor recognition by a calicivirus. J Am Chem Soc 130:3669–3675

Ramirez B, Antanasijevic A, Caffrey M (2014) Ligand screening using NMR. Methods Mol Biol 1140:305–313

Schlünzen F, Zarivach R, Harms J, Bashan A, Tocilj A, Albrecht R, Yonath A, Franceschi F (2001) Structural basis for the interaction of antibiotics with the peptidyl transferase centre in eubacteria. Nature 413:814–821

Shuker SB, Hajduk PJ, Meadows RP, Fesik SW (1996) Discovering high-affinity ligands for proteins: SAR by NMR. Science 274:1531–1534

Sowell J, Mason JC, Strekowski L, Patonay G (2001) Binding constant determination of drugs toward subdomain IIIA of human serum albumin by near-infrared dye-displacement capillary electrophoresis. Electrophoresis 22:2512–2517

Williamson MP (2009) Chapter 3 Applications of the NOE in molecular biology. In: Webb GA (ed) Annual reports on NMR spectroscopy, Vol 65. Academic Press, pp 77–109